Molecular Model for the Mechanical Properties of Elastomers. 4. Interpenetrating Networks

Yves Termonia

Central Research and Development, Experimental Station, E. I. du Pont de Nemours, Inc., Wilmington, Delaware 19898

Received May 22, 1990; Revised Manuscript Received August 23, 1990

ABSTRACT: The ultimate mechanical properties of simultaneous and sequential interpenetrating networks (IPNs) have been studied theoretically. Results for bimodal networks made through interpenetration of long by very short PDMS chains show no synergism in mechanical properties. Tensile strength and toughness values for IPNs are usually lower than those for the corresponding interconnected networks. Based on our model results, a new type of IPN is proposed in which the long chains form macrocycles which are threaded by the short-chain component. Those novel IPNs show very high toughness values which are comparable to those of the interconnected bimodal networks. Finally, our study indicates that network dominance in a sequential IPN is due to the lower extensibility of the earlier polymerized network and not, as previously anticipated, to segregation of the later polymerized monomer.

1. Introduction

There is at present a wide interest in the use of multipolymer combinations for producing advanced polymeric material with outstanding mechanical properties. Such combinations include mechanically blended polymers as well as graft and block copolymers. Special attention has also been devoted recently to interpenetrating polymer networks (IPNs) made by cross-linking one polymer in the immediate presence of another (for an excellent review, see ref 1).

Two types of IPNs are possible.[1] In the simultaneous IPN, polymers I and II are mixed together with their respective cross-linkers. The two components are then cured simultaneously via noninteracting cross-linking reactions. In the sequential IPN, one starts by cross-linking polymer I. A solution of polymer II with its own cross-linking agent is then swollen into polymer I and cured in situ.

Most experimental studies of IPNs have focused on heterogeneous systems made through cross-linking a rubbery and a glassy polymer.[2,3] The interest in those combinations stems from the possibility of producing a whole series of new materials ranging from a filler-reinforced elastomer to a rubber-reinforced plastic. The mechanical properties of those materials are however mainly controlled by the detailed morphology of their two-phase nature, which is itself dependent on the mode of mixing. Thus, these studies are unable to address basic questions such as the importance of the mode of cross-linking (sequential vs simultaneous) or the possibility of domination of one network over the other.

A fundamental understanding of these issues has to be obtained through the use of homo-IPNs in which polymers I and II are identical from a chemical point of view. Experimental swelling studies and analysis of modulus data of sequential homo-IPNs have successfully demonstrated the domination of network I over network II.[4-6] More recently, Mark et al.[7] have made a detailed investigation of the stress–strain data of IPNs formed through end-linking of long and short poly(dimethylsiloxane) chains. These studies clearly illustrate the basic differences between simultaneous and sequential IPNs from a mechanical point of view. The purpose of the present work is to complement those experimental results with those of a model network in which the effects of molecular weight, entanglements, and mode of cross-linking are explicitly taken into account. As in ref 7, this paper is devoted to the study of IPNs made of blends of short with very long molecular chains. The interest in those networks arises from the possibility of producing new materials with properties encompassing the advantages of both molecular weight components, i.e., high stiffness and high elongation at break.

2. Model

Our model is based on previous theoretical work on PDMS cross-linked networks, described at length in refs 8 and 9. The essential features of interest for the present purposes will briefly be summarized here. As in our study of interconnected bimodal networks,[9] the long PDMS chains (network I) are given a molecular weight $M_I = 4M_e$, in which M_e denotes the molecular weight between entanglements. For the short chains (network II), we choose $M_{II} = M_e/4$. The number of statistical segments for the short chains equals 2, whereas that for M_e is 8. This is a convenient feature[9] which sets the distance between successive entanglements in the undeformed network equal to twice the length of the end-to-end vector for the short chains. Since we will be concerned only with ultimate mechanical properties of bimodal IPNs, we assume an ideal intimate mixture of the two molecular weight components. This, in effect, leads to maximization of the number of entanglements formed through interpenetration of networks I and II. For the purpose of simplicity, the present work is restricted to the case of two-dimensional networks.

(a) Simultaneous IPN. Figure 1 shows a typical simultaneous IPN, as obtained from our approach, prior to deformation. The network is for a 37% weight fraction of the long chains. The long chains are represented by the heavy dark lines and have each four entanglements (symbols ●) along their contour. The short chains, on the other hand, are represented by the light lines bounded between successive tetrafunctional cross-links (symbols □). Note the perfect interpenetration of networks I and II, which entangle along their boundaries.

The simultaneous IPNs are obtained on a computer as follows. We start with a two-dimensional square lattice having unit length equal to the end-to-end vector length of the short chains. The long-chain network I is then generated by a series of random walks of 4 steps each ($M_I = 4M_e$), each step having a length equal to that between

0024-9297/91/2224-1392$02.50/0

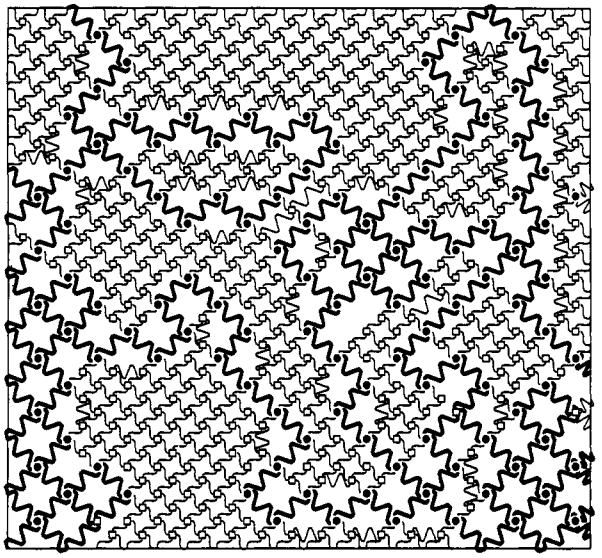

Figure 1. Typical simultaneous IPN before deformation, as obtained in the present model. The network is made of a bimodal distribution of long and very short molecular chains. The long chains (heavy dark lines) have a molecular weight $M_I = 4M_e$, in which M_e is the molecular weight between entanglements. For the short chains (light lines), we take $M_{II} = M_e/4$. The figure is for a 37% weight fraction of the long chains and a degree of advancement of the reaction $p = 1$. Symbols are as follows: (●) entanglement; (□) tetrafunctional cross-link.

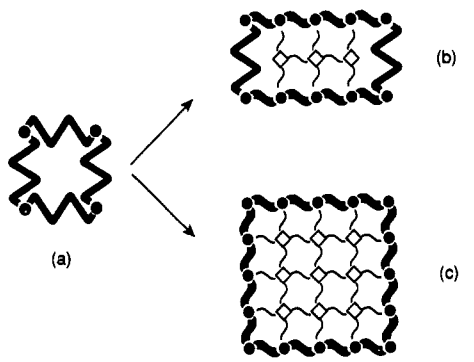

Figure 2. Model representation of the swelling of network I: (a) unswollen element; (b) swollen element containing 50% short chains II; (c) swollen element with 75% short chains II. Notation is the same as in Figure 1.

entanglements, viz., 2 unit lattice lengths (see above). In order to ensure an optimum cross-linking efficiency for network I, every new chain I is started at a site adjacent to the end of a previously generated chain. When a prescribed weight fraction is reached, the building up of network I is stopped and the unassigned lattice bonds are filled in with the short chains. Chain ends belonging to the same polymer species (I or II) are then made to react with probability p.

(b) Sequential IPN. In a sequential IPN, we start by generating the network I of long chains, as for the simultaneous case. Here, however, the generation of random walks of 4 steps proceeds until the whole lattice is filled in. Chain ends in network I are then cross-linked with probability p. Figure 2a schematically depicts the repetition unit of network I. Upon swelling by chains II, that unit will deform and turn into units b and c in Figure 2 which contain respectively 50 and 75% polymer II network. As stated above, we assume perfect interpenetration of the two networks, which entangle at their points of contact. Note also that, as in unit a, chain strands between junctions (entanglements and cross-links) in both units b and c are in mechanical equilibrium; i.e., their end-to-end vector length is proportional to the square root of the number of statistical segments. That attainment of mechanical equilibrium under conditions of perfect interpenetration is unique to structures b and c. The sequential IPNs were thus obtained from the pure I network by judiciously replacing (along diagonal lines; see Figure 3) some of its units (Figure 2a) by the swollen elements (Figure 2b,c) until the desired weight fraction of polymer II is attained. Note that this procedure leads to the assumption of a nonhomogeneous swelling of network I upon the addition of the short chains II, a situation which is probably also the case experimentally. Figure 3a gives our representation of a sequential IPN with 57% long chains; Figure 3b is for 25% long chains, corresponding to the limit of a network made solely of the unit appearing in Figure 2c.

Figures 1–3 are for the case of fully reacted cross-links, $p = 1$. In practical situations, however, $p < 1$. This leads to the presence in the IPN of cross-links with only one or zero reacted ends. The latter are not elastically active and therefore need to be removed from the network. Additional attention also has to be paid to entanglement points which, because of an incompleteness of the reaction, are not trapped between cross-links. These also need to be removed since they do not contribute to the mechanical properties of the network *at elastic equilibrium*.

Upon completion of the construction of an IPN and removal of the non-load-bearing junctions, the mechanical properties are tested as follows (for more details, see refs 8 and 9). The two dimensional (x,y) network is stretched along the y axis in a series of small strain increments. For each value of the external strain, the network is relaxed to its minimum-energy configuration through a series of fast computer algorithms which steadily reduce the net residual force acting on each network junction. The force f on a particular chain strand between two junctions is calculated by using the classical treatment of rubber elasticity

$$f = (kT/l)\,\mathcal{L}^{-1}(\mathbf{r}/nl) - f_0 \qquad (1)$$

in which $\mathbf{r}$ and n denote, respectively, the length of the end-to-end vector and the number of statistical segments (of length l) for the strand. $\mathcal{L}^{-1}$ is the inverse Langevin function, whereas f_0 denotes the local force in the absence of strain, i.e., that for which $\mathbf{r} = n^{1/2}l$.[8] The nonaffine displacements of those junctions create large force gradients on chains passing through trapped entanglements. These gradients then lead to the possibility of chain slippage, which is allowed in the model until the difference in force in the two strands of a chain separated by an entanglement falls below an entanglement friction force denoted by f_e (in kT/l units). The latter, which is expected to be temperature dependent, fully controls the extent of entanglement slippage: for $f_e > 100$, chain motion through entanglements is frozen-in whereas at $f_e = 0$, chains slip freely past each other. Henceforth, we set $f_e = 0.01$. That choice of value leads to a moderate amount of chain slippage and is not expected to affect the conclusions of the present paper.

3. Results and Discussion

Figure 4 shows a series of calculated stress–strain curves for simultaneous IPNs at various weight fractions of the high molecular weight component I. The degree of advancement of the cross-linking reaction was set equal to $p = 0.95$ for both long and short chains. The stress–strain curves for the pure components I and II are denoted by dashed lines. As in the case of conventional bimodal

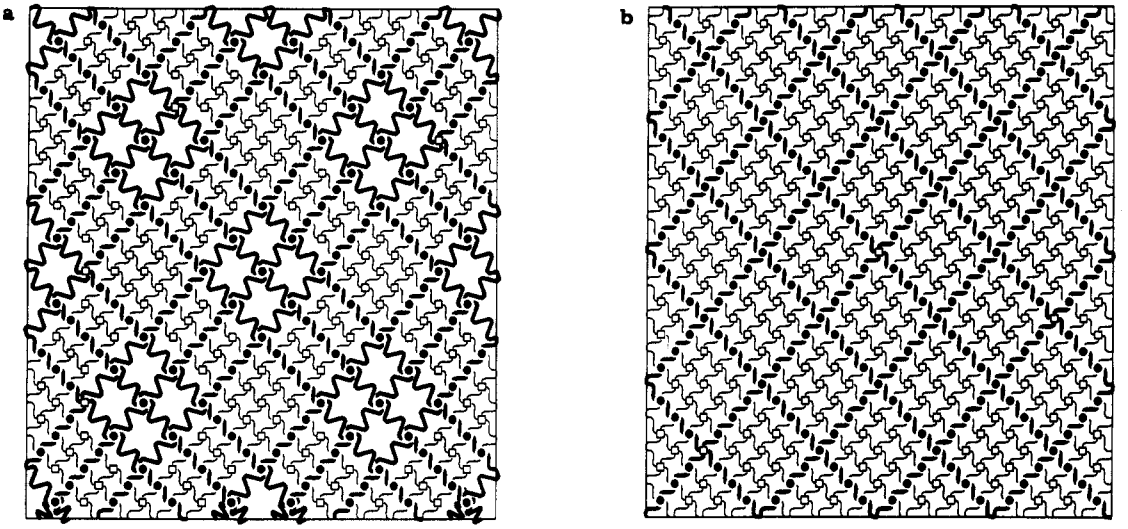

Figure 3. Typical sequential IPNs before deformation, as obtained in the present model: (a) 57% long chains; (b) 25% long chains. Notation is the same as in Figure 1.

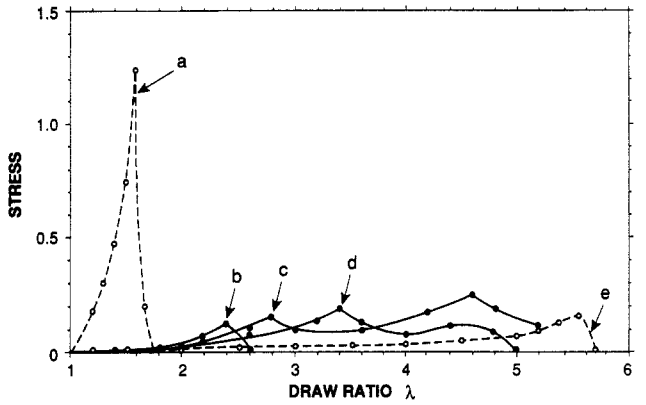

Figure 4. Calculated stress–strain curves for simultaneous IPNs. The stress is in arbitrary units. The curves are for different values of the weight fraction of the high molecular weight component: curve a, 0%; curve b, 54%; curve c, 64%; curve d, 72%; curve e, 100%. The degree of advancement of the cross-linking reaction was set equal to $p = 0.95$ for both long and short chains. The figure is for the case of chain slippage with an entanglement friction force[8,9] $f_e = 0.01$ (in kT/l units).

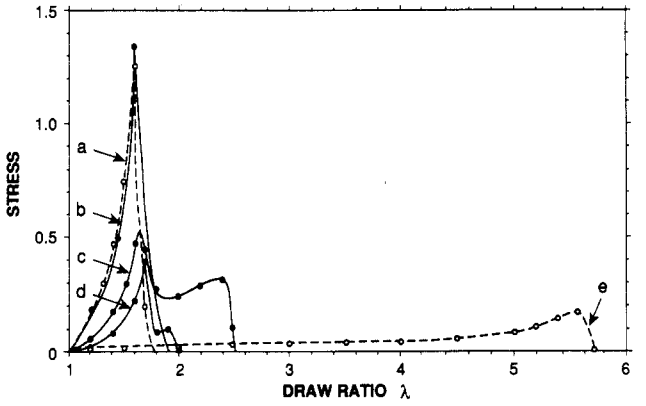

Figure 5. Same as Figure 4 but for sequential IPNs: curve a, 0%; curve b, 25%; curve c, 57%; curve d, 77%; curve e, 100%.

cross-linked networks,[9] intermediate compositions (see curves c and d) show the presence of two well-defined peaks. The peak at low strain corresponds to hardening and fracture processes involving the low molecular weight component II; that at higher strain relates to similar effects for the long-chain component I. In all cases, the stress values reached in the simultaneous IPNs are much lower than those for the conventional bimodal networks.[9] The reason for those poor mechanical properties lies in the absence of chemical cross-linking between chains I and II in the IPN. Further study shows that this lack of connectivity leads at 54% long chains (curve b) to a network I with a large fraction of elastically inactive dangling ends. This in turn results in a sharp drop in the elongation at break ($\lambda_{break} = 2.6$; see Figure 4) and a control of the properties by network II.

Our calculated results for sequential IPNs are presented in Figure 5. The stress–strain curves for the blends (curves b–d) exhibit a much higher modulus and lower elongation at break than those for the simultaneous IPNs (Figure 4). The reason for that markedly different behavior is twofold. First, in contrast to the case of Figure 4, network I in a sequential IPN extends throughout the system (Figure 3), which leads to better connectivity between chains I. This results, at equal blend compositions, to a much larger fraction of elastically active chain strands in sequential than in simultaneous IPNs (65% for curve c, Figure 5, vs 42% for curve b, Figure 4). Second, due to their prior swelling, chains I in a sequential IPN have a lower extensibility, leading to higher stress and smaller elongation at break.

From the above considerations, it transpires that high toughness in an IPN requires the long-chain network to have the least amount of dangling ends and no loss in extensibility due to prior swelling. These conditions can be obtained in a simultaneous IPN in which the long chains have a propensity to form macrocycles upon cross-linking. An example would be long diester chains which form acyloin rings in the presence of sodium and acetic acid.[10] Another way of forming macrocycles would be to decrease the functionality of the cross-linker for the long chains, viz., from a tetra- to a bifunctional element. The threading of these rings by the short chains leads to the formation of so-called rotaxanes. A typical IPN in which the long-chain network (network I) is made of an ensemble of macrocycles is illustrated in Figure 6. In that figure, the long chains cross-link (with $p = 0.95$) in groups of 4 units to form rings which are then entangled with the short-chain network II.

Figure 7 shows a series of calculated stress–strain curves for the networks of Figure 6. The curves (b–d) for the networks containing the rotaxanes are quite different from those obtained in conventional IPNs (Figures 4 and 5). The threaded-ring conformation of the high molecular weight component now leads to much higher toughness

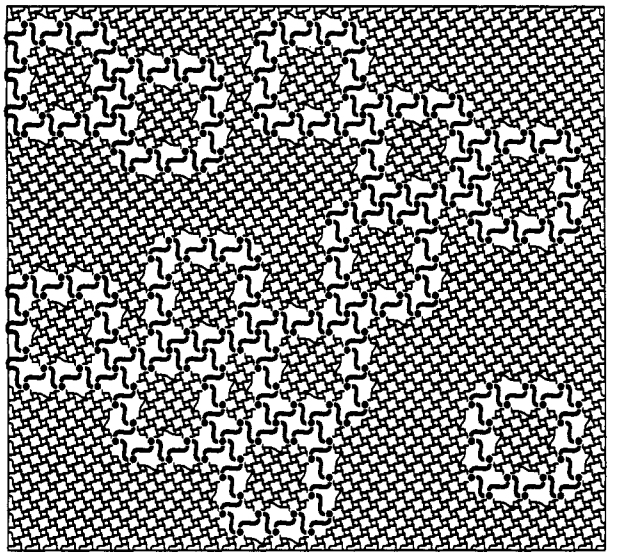

Figure 6. Interpenetrating polymer network containing rotaxanes. The long chains (heavy dark lines) associate in groups of four units to form closed macrocycles. The figure is for a 23% weight fraction of the long chains and a degree of advancement of the reaction $p = 1$. Notation is the same as in Figure 1.

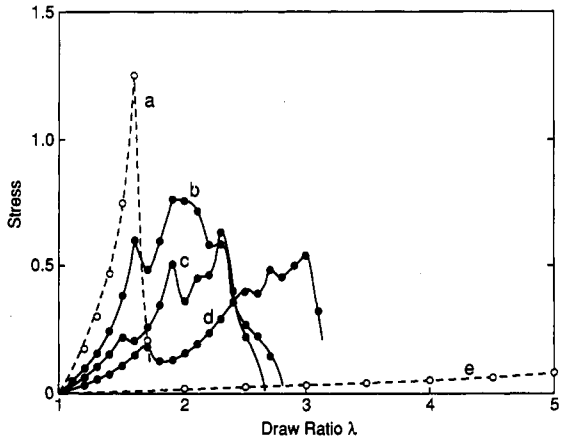

Figure 7. Calculated stress–strain curves for the networks of Figure 6. Notation is the same as in Figure 4. Curve a, 0%; curve b, 17%; curve c, 23%; curve d, 37%; curve 3, 100%.

values which actually are comparable to those observed in the corresponding interconnected bimodal networks.[9] This, in turn, confirms our conjecture (see above) that the poor mechanical properties in conventional simultaneous IPNs (Figure 4) are due to the lack of connectivity between the long chains.

We now turn to a study of the possible dominance of one network over the other in a sequential IPN. To this end, we assign to chains I and II different cross-linking probabilities henceforth denoted by p_I and p_{II}, respectively. Figure 8a shows the dependence of tensile strength on p_I at constant $p_{II} = 0.95$ for a 57% weight fraction of the long chains. Figure 8b is for a constant $p_I = 0.95$ and varying p_{II}. Figures 8a,b clearly show that *both* p_I and p_{II} control the mechanical properties and there is no dominance of one network over the other. These conclusions are at variance with experimental observation.[1,5] It should be noted, however, that our results in Figure 8 are for sequential IPNs in which chains I and II are of *different* lengths, whereas the results in refs 1 and 5 are for a unimodal length distribution of I and II chains. That difference is of importance because in the former case, the swollen network I, being made of the long chains, ends up in the IPN with an elongation at break comparable to that

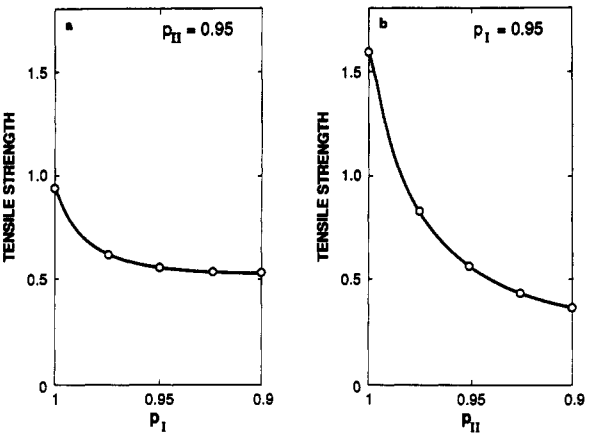

Figure 8. Dependence of tensile strength on the cross-linking probabilities p_I and p_{II} for chains I and II, respectively. The figure is for the bimodal sequential IPNs studied in Figure 5 with 57% long chains. (a) $p_{II} = 0.95$, p_I varies; (b) $p_I = 0.95$, p_{II} varies.

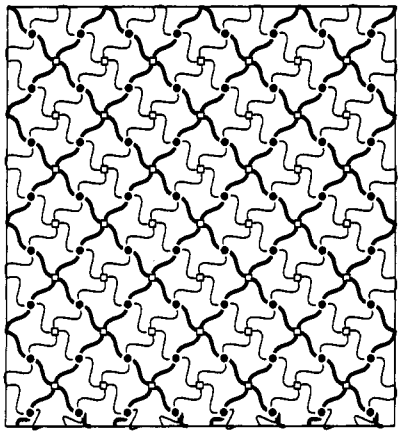

Figure 9. Sequential IPN in which chains I and II are given the same initial length. Network I (heavy lines), being in a swollen state, is given a low 70% elongation at break. Network II (thin lines) breaks at a much higher 130% elongation.

of the short-chain network II (see also Figure 5 in that connection). In the case of a unimodal length distribution, on the other hand, the elongation at break of chains I in the IPN is much smaller than that of chains II. We now turn to show, with the help of our approach, that the latter can fully account for a network I dominance, as observed experimentally in refs 1 and 5.

Our model for a sequential IPN made of a uniform length distribution of I and II chains is schematically represented in Figure 9. Network I (heavy lines), being in a swollen state, is given a low elongation at break around 75%. For network II, we choose a 125% break elongation. Our results for the dependence of maximum tensile strength on p_I and p_{II} are presented in Figure 10. The figure clearly shows a strong effect of p_I at constant p_{II} (Figure 10a), whereas mechanical properties appear to be unaffected by any change in p_{II}, keeping p_I constant. These two sets of observations clearly point to the dominance of the IPN properties by those of network I. Our study in turn indicates that this effect can be fully explained in terms of the shorter elongation at break of the swollen network I without the need to invoke[5] greater continuity of network I and segregation of chains II. Note also that segregation effects should be of secondary importance in view of our results of Figure 8 which were themselves for a partially segregated IPN (Figure 3a).

To conclude, we have presented a detailed molecular model for the description of the factors controlling the

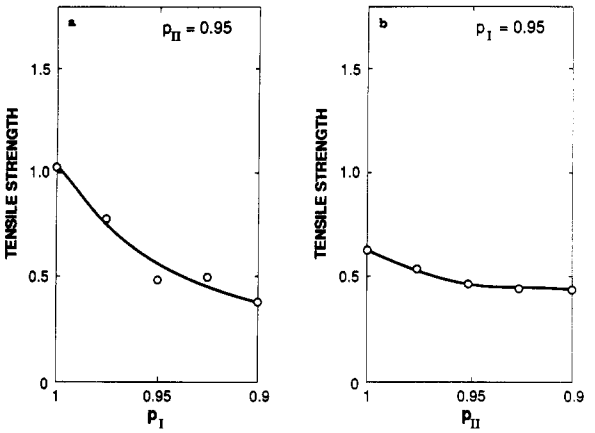

Figure 10. Dependence of tensile strength on the cross-linking probabilities p_I and p_{II} for chains I and II, respectively. The figure is for the network presented in Figure 9 in which chains I and II have the same initial length. (a) $p_{II} = 0.95$, p_I varies; (b) $p_I = 0.95$, p_{II} varies.

mechanical properties of interpenetrating networks made of short and long flexible chains. The model clearly indicates that the poor mechanical properties in simultaneous IPNs are due to a lack of connectivity among the long chains. In a sequential IPN, on the other hand, prior swelling of the long chains has a deleterious effect on the elongation at break. On the basis on those observations, our model points to possible advantages of a new type of IPN in which the long chains form macrocycles which are threaded by the short-chain component. It should be noted that the conclusions of the present paper are based on two-dimensional model networks for which the radius of gyration r_g and that, r_v, of the volume occupied by a chain strand both scale like $n^{1/2}$, in which n is the number of statistical segments for the strand. In an actual three-dimensional network, this is not the case since $r_v \sim n^{1/3}$. An extension of the present model results to actual 3-dimensional networks is in progress.

References and Notes

(1) Sperling, L. H. *Interpenetrating Polymer Networks and Related Materials*; Plenum Press: New York, 1981.
(2) Bucknall, C. B. *Toughened Plastics*; Applied Science Publishers: London, 1977.
(3) Frisch, K. C.; Klempner, D.; Frisch, H. L. *Polym. Eng. Sci.* **1982**, *22*, 17.
(4) Millar, J. R. *J. Chem. Soc.* **1960**, 1311.
(5) Siegfried, D. L.; Manson, J. A.; Sperling, L. H. *J. Polym. Sci., Polym. Phys. Ed.* **1978**, *16*, 583.
(6) Thiele, J. L.; Cohen, R. E. *Polym. Eng. Sci.* **1979**, *19*, 284.
(7) Mark, J. E.; Ning, Y.-P. *Polym. Eng. Sci.* **1985**, *25*, 824.
(8) Termonia, Y. *Macromolecules* **1989**, *22*, 3633.
(9) Termonia, Y. *Macromolecules* **1990**, *23*, 1481.
(10) Wasserman, E. *Sci. Am.* **1962**, *2075*, 94.